Synthesis, thermal processing, and thin film morphology of poly(3-hexylthiophene)-poly(styrenesulfonate) block copolymers

H. Erothu, J. Kolomanska, P. Johnston, S. Schumann, D. Deribew, D.T.W. Toolan, Alberto Gregori, Christine Lartigau-Dagron, G. Portale, W. Bras, et al.

Synthesis, Thermal Processing and Thin Film Morphology of Poly(3-Hexylthiophene)-Poly(Styrene Sulfonate) Block Copolymers

*Harikrishna Erothu,[1] Joanna Kolomanska,[1] Priscilla Johnston,[1] Stefan Schumann,[2] Dargie Deribew,[3] Daniel T. W. Toolan,[4] Alberto Gregori,[5] Christine Dagron-Lartigau,[5] Giuseppe Portale,[6] Wim Bras,[6] Thomas Arnold,[7] Andreas Distler,[3] Roger C. Hiorns,[8] Parvaneh Mokarian-Tabari,[9,10] Timothy W. Collins,[9] Jonathan R. Howse,[4] and Paul D. Topham[1]**

1. Chemical Engineering and Applied Chemistry, Aston University, Birmingham, B4 7ET, UK.

2. Heraeus Deutschland GmbH & Co. KG, Business Line Display and Semiconductors (HNB), Chempark Leverkusen / Gebäude B 202, D-51368 Leverkusen, Germany.

3. Belectric OPV GmbH, Landgrabenstr. 94, 90443 Nürnberg, Germany.

4. Department of Chemical and Process Engineering, University Of Sheffield, Sheffield, S1 3JD, UK.

5. Institut des Sciences Analytiques et de Physico-chimie pour l'Environnement et les Matériaux (IPREM) UMR 5254, Université de Pau et des Pays de l'Adour, 64053 Pau, France.

6. Netherlands Organisation for Scientific Research, DUBBLE@ESRF Beamline BM26, ESRF - The European Synchrotron, 71, Avenue des Martyrs, CS 40220, 38043, Grenoble Cedex 9, France.

7. I07 Beamline, Diamond Light Source Ltd, Harwell Science and Innovation Campus, Didcot, OX11 0DE, UK.

8. CNRS, Institut Pluridisciplinaire de Recherche sur l'Environment et les Materiaux (IPREM UMR 5254), 64053 Pau, France.

9. Department of Chemistry, University College Cork and Tyndall National Institute, Cork, Ireland.

10. Centre for Research on Adaptive Nanostructures and Nanodevices (CRANN) and AMBER Centre, Trinity College Dublin, Dublin, Ireland.

KEYWORDS. Poly(3-hexylthiophene), poly(*p*-styrene sulfonate), block copolymer, self-assembly, SAXS/WAXS, RAFT, GRIM, click chemistry, organic photovoltaics

ABSTRACT

A series of novel block copolymers, processable from single organic solvents and subsequently rendered amphiphilic by thermolysis, has been synthesized using Grignard Metathesis (GRIM) and Reversible Addition-Fragmentation chain Transfer (RAFT) polymerizations and azide-alkyne click chemistry. This chemistry is simple and allows the fabrication of well-defined block copolymers with controllable block lengths. The block copolymers, designed for use as interfacial adhesive layers in organic photovoltaics to enhance contact between the photoactive

and hole transport layers, comprise printable poly(3-hexylthiophene)-*block*-poly(neopentyl *p*-styrene sulfonate), P3HT-*b*-PNSS. Subsequently, they are converted to P3HT-*b*-poly(*p*-styrene sulfonate), P3HT-*b*-PSS, following deposition and thermal treatment at 150 °C. Grazing incidence small and wide angle x-ray scattering (GISAXS/GIWAXS) revealed that thin films of the amphiphilic block copolymers comprise lamellar nanodomains of P3HT crystallites that can be pushed further apart by increasing the PSS block lengths. The approach of using a thermally-modifiable block allows deposition of this copolymer from a single organic solvent and subsequent conversion to an amphiphilic layer by non-chemical means, particularly attractive to large scale roll-to-roll industrial printing processes.

INTRODUCTION

Organic photovoltaics (OPVs) have attracted significant attention in recent years, due to several redeeming features such as being extremely thin, flexible and lightweight alongside their inherently simple solution-based manufacturing process.[1-5] On the other hand, the main disadvantage, that of instability, limits the commercialization of these next generation solar cells. Extensive research in the OPV area is currently focused on increasing OPV lifetime by introducing new materials,[6-10] improvements in the manufacturing process[11-13] and elimination/suppression of material degradation.[14-17] A range of degradation mechanisms has already been determined, including oxygen and water diffusion into the device,[16, 18, 19] breakdown of active material,[16, 20, 21] electrode and interlayer diffusion[16, 22, 23] and reactions of the electrode(s) with the organic layers.[16, 24] Alongside morphological instability of the materials within the device,[16, 20, 21] macroscopic degradation, such as delamination, is also observed.[16, 20, 25] Charge generation and transport in OPVs are strongly dependent on morphology and phase

behaviour of employed materials,[26-28] therefore advanced control at the nanoscale level is crucial. Recently, extensive studies of the introduction of block copolymers into OPV devices have been reported.[29, 30] The use of block copolymers in OPVs can be divided into three groups: compatibilizers,[29-33] templating agents[29, 34, 35] and active materials.[29, 30, 36, 37] The application of block copolymers in the photoactive layer limits macrophase separation of the donor (D) and acceptor (A), avoiding this particular aspect of device performance loss over time. For example, block copolymer compatibilizers reduce the interfacial energy between donor and acceptor and thus limit domain coarsening. In these strategies, poly(3-hexylthiophene (P3HT, the most commonly studied donor polymer) and [6,6]-phenyl-C_{61}-butyric acid methyl ester (PCBM, the most studied acceptor, particularly in conjunction with P3HT) have been widely explored in rod-coil block copolymers.[38, 39] Only a limited number of reports on exclusively D-A rod-rod copolymers have been published; a consequence of complicated synthetic procedures,[40] however several groups have reported the incorporation of P3HT into π-conjugated systems.[41-43]

Copolymers comprising a P3HT rod block and a non-conductive coil block have particularly attracted significant interest.[39, 44] In this regard, the development of controlled-radical polymerization procedures, specifically atom transfer radical polymerization (ATRP), nitroxide-mediated polymerization (NMP) and reversible addition-fragmentation chain transfer (RAFT) polymerization, has been instrumental in the design of non-conjugated coils grown from a readily end-functionalized P3HT macroinitiator, or macroCTA (chain transfer agent) for RAFT. The alternative synthetic route is a coupling reaction between two end-functionalized homopolymers. Both strategies have been explored to synthesize various compatibilizers based on P3HT, such as P3HT-*b*-polyethylene (P3HT-*b*-PE),[45-47] P3HT-*b*-poly(ethylene oxide) (P3HT-

b-PEO),[48-51] P3HT-*b*-poly(methyl methacrylate) (P3HT-*b*-PMMA)[47, 52, 53] and P3HT-*b*-polystyrene (P3HT-*b*-PS).[54]

While P3HT is explored mostly in the organic electronics field, poly(*p*-styrene sulfonate), PSS, is exploited in a wider range of applications such as water softening,[55] medicine,[56, 57] biomaterials,[58] and fuel cells.[59] One of the most important uses of PSS is as a counter-ion polymer to complex and electronically stabilize poly(3,4-ethylenedioxythiophene) (PEDOT) in organic electronic devices. PEDOT:PSS is applied in organic photovoltaics (OPVs) as a hole conducting 'buffer' layer[4, 60-62] and in organic light emitting diodes (OLEDs) as a hole injection layer.[63, 64] Recently, the complex has been also explored as a possible electrode replacement for indium tin oxide (ITO).[65, 66] However, the highly polar character of PSS limits its further incorporation into apolar conducting systems, which are processed from organic solvents, such as those comprising polythiophenes,[67, 68] polycarbazoles[69, 70] and/or fullerene derivatives.[68, 71]

In this contribution, the design, synthesis, and molecular and morphological characterization of a new block copolymer, P3HT-*b*-PSS, is reported. The motivation to synthesize and study this block copolymer is the need to enhance contact between the photoactive and hole transport layers (PAL and HTL, respectively) within an OPV device. This interface suffers from delamination over time owing to the differing surface energies of the adjacent layers, which leads to a breakdown in device performance.[25] Our new polymer is designed for use as an interfacial layer between the PAL and HTL, with the P3HT block enhancing adhesion with the P3HT in the PAL and the PSS taking part in electrostatic interactions with the PEDOT:PSS complex in the HTL. However, owing to its amphiphilic character, it is difficult to obtain a common solvent for this block copolymer, which is essential for homogeneous deposition during

the manufacturing process. Additionally, to enable the synthesis of the copolymer, a common solvent is preferable to link the two blocks together. A more conventional approach is to use polystyrene and subsequently sulfonate the aromatic rings using sulfuric acid. The problems with this route are; (i) it is difficult to control to level of sulfonation; and (ii) this chemical modification would have to take place within the device post deposition.

An alternative solution is the introduction of a protecting entity on the sulfonate group to render the PSS organophilic, enabling the synthesis and deposition of the block copolymer from a single organic solvent. To restore the polar properties of PSS, the protecting group can be removed after material deposition. However, traditional methods relying on chemical washing, such as catalyzed hydrolysis, should be avoided since components within a given system or device could be damaged or removed by the 'wet' processing route. Additionally, production of chemical waste and difficulties in industrial scale washing processes limit the use of the chemical deprotection procedure in roll-to-roll printing. Therefore, the development of a more suitable alternative method is highly desirable. Thermal removal of the protecting group is a potential solution to the aforementioned issues; however it is not without its drawbacks. For example, it is known that sustained high temperature treatment leads to the degradation of OPV materials and loss in solar cell performance (particularly important for inverted devices).[72, 73] Hence, the protecting group should be cleavable within a short time period at suitably low temperature; the precise upper limit of this treatment being dictated by the materials used in the underlying layers (including substrate) within the device. Identified in the work of Baek *et al.*[74, 75] and explored by Thelakkat's group,[76] the neopentyl group has been chosen herein as the thermally-labile protecting group of PSS. RAFT polymerization, well known for the controlled synthesis of well-defined polymers from a wide-range of monomers,[77-83] has been employed to afford azide-

functionalized poly(neopentyl *p*-styrene sulfonate) (PNSS-N_3) of varying chain lengths. Simultaneously, ethynyl-terminated P3HT has been synthesized via GRIM polymerisation, an extremely efficient route for polymerising conductive thiophene monomers.[84] PNSS-N_3 was subsequently coupled to ethynyl-P3HT via copper-catalyzed click chemistry in an organic solvent.[85-87]

Thermal deprotection of the P3HT-PNSS block copolymers has been monitored by thermogravimetric analysis (TGA) and subsequent microphase separation and crystallization of thin films has been characterized by grazing incidence small and wide angle x-ray scattering (GISAXS/GIWAXS) and atomic force microscopy (AFM). The results herein provide the synthetic route to a family of completely novel block copolymers (as shown in Scheme 1) and outline relevant processing conditions to produce microphase separated thin films from these new amphiphilic materials. Furthermore, we introduce a route for the design of thermally-modifiable block copolymers for use in applications, such as organic electronics, which rely on facile roll-to-roll processing for low cost device manufacture.

EXPERIMENTAL PART

MATERIALS

tert-Butylmagnesium chloride (^{t}BuMgCl, 1 M solution in tetrahydrofuran, THF), 1,3-bis(diphenylphosphino) propane nickel(II) chloride [Ni(dppp)Cl_2], ethynylmagnesium bromide (0.5 M solution in THF), CuI (95 %), diisopropylethylamine (DIPEA), anhydrous anisole (HPLC) and anhydrous THF, were purchased from Sigma Aldrich and used without further purification. 2,2′-Azobis(isobutyronitrile) (AIBN) was purchased from TCl and used as supplied. THF (HPLC), chloroform (HPLC), acetone, methanol, propan-2-ol and hexane, (Laboratory

Grade) from Fisher scientific, were all used as received. Neutral aluminium oxide, Brockmann I, 50 – 200 μm was purchased from Acros Organics. P3HT (M_w = 40 kg mol^{-1}, $Đ$ = 1.49) and PC[60]BM were purchased from Merck Chemicals Ltd and Solenne, respectively, and used as received. PEDOT:PSS (Clevios PAI 4083) was obtained as an aqueous dispersion from Heraeus Precious Metals and used as received. Monomer, 2,5-dibromo-3-hexylthiophene,[88] azide-terminated chain transfer agent, 2-dodecylsulfanylthiocarbonylsulfanyl-2-methyl propionic acid 2-azido-ethyl ester (CTA-N_3),[89] and neopentyl *p*-styrene sulfonate (NSS) monomer,[90] were synthesized according to literature procedures.

METHODS

Synthesis of ethynyl-terminated regioregular poly(3-hexylthiophene) (P3HT$_{50}$-ethynyl), 2

In a dry, three necked round-bottomed flask, flushed with nitrogen, 2,5-dibromo-3-hexylthiophene (**1**, 6.05 g, 18.5 mmol) was dissolved in anhydrous THF (40 mL) and stirred under nitrogen for 15 minutes. Afterwards, tert-butylmagnesium chloride (18.5 mL, 18.5 mmol, 1 M in THF) was added via syringe under nitrogen and the reaction mixture was stirred at room temperature for 2.5 h. The solution was further diluted with 160 mL of anhydrous THF, before Ni(dppp)Cl_2 (0.125 g, 0.230 mmol) was added in one portion and the reaction mixture stirred for 45 minutes at room temperature. Ethynylmagnesium bromide (14.8 mL, 14.8 mmol, 0.5 M in THF) was then added via syringe to the reaction mixture and stirred for an additional 45 minutes. Finally, the crude polymer product was precipitated into methanol (800 mL) and then purified by dissolving in chloroform, filtering, and then reprecipitating the polymer in methanol several times to yield alkyne-functionalized P3HT. The polymer was dried overnight under vacuum and finally stored under inert atmosphere, protected from light. ^{1}H NMR (300 MHz, $CDCl_3$, ppm): δ

= 6.98 (s, 1nH), 3.52 (s, 1H), 2.80 (t, 2nH), 1.70 (m, 2nH), 1.34-1.43 (m, 6nH), 0.91 (t, 3nH). FTIR: 2800-3000 cm^{-1} (C-H), 3310 cm^{-1} (≡C-H), 2095 cm^{-1} (C≡C). From ^{1}H NMR, the number-average degree of polymerisation, D_p, was calculated to be approximately 50 (see discussion), and regioregularity (RR) ~ 96 %.

Synthesis of azide-terminated poly(neopentyl *p*-styrene sulfonate) (PNSS-N_3), 4

PNSS-N_3 (**4**) was synthesized according to a literature procedure with a slight modification.[76, 91] Herein, PNSS-N_3 was synthesised by RAFT polymerization using AIBN and CTA-N_3 in anisole at 80 °C, as shown in Scheme 1.

The following procedure describes the synthesis of PNSS-N_3 with a target degree of polymerization of 10, but is representative of all PNSS syntheses (with the major difference between protocols being the $[NSS]_0/[CTA\text{-}N_3]_0$ ratio, see ESI, Table S1). In a 50 mL flame-dried round-bottomed flask, NSS (**3**, 5.056 g, 19.6 mmol, 10 eq.), AIBN (0.064 g, 0.393 mmol, 0.2 eq.), CTA-N_3 (0.853 g, 1.96 mmol, 1 eq.) and anhydrous anisole (5 mL, 50 % w/v solution) were added. The flask was degassed by continuous purging of Ar gas through the reaction mixture for 30 minutes. Following which, the flask was immersed into a preheated oil bath at 80 °C and the polymerization was allowed to proceed for approximately 26 h. The reaction was stopped by immersing the flask into an ice bath. To remove unreacted material, the reaction mixture was diluted with chloroform and reprecipitated in hexane (twice), before being was dried under vacuum for overnight. Yield: 4.18 g. ^{1}H NMR in $CDCl_3$ (δ, ppm): 7.72 (br, 2H, Ph); 7.2 (br, 5H, Ph); 6.65 (br, 2H, Ph); 5.3 (s, 2H, C**H₂**-Ph); 4.3 (br, 2H, O-C**H₂**); 3.75 (br, 2H, -S-O-C**H₂**); 3.65 (CS-C**H₂**); 3.48 (br, 2H, C**H₂**-N_3); 2.75 (br, 2H, COO-C**H₂**); 1.75 (br, 1H, C**H**-Ph); 1.4 (br, 2H, C**H₂**-CH); 0.91 (br, 9H, (C**H₃**)$_3$. FTIR: 2100 cm^{-1} (-N=N=N), 2800-3000 cm^{-1} (C-H).

Synthesis of poly(3-hexylthiophene)-*block*-poly(neopentyl *p*-styrene sulfonate) (P3HT-*b*-PNSS)

In a typical experiment for the synthesis of $P3HT_{50}$-*b*-$PNSS_9$ (conditions used for the synthesis of other blocks are provided in the ESI, Table S2); P3HT-ethynyl, **2** (250 mg, 0.03 mmol, 1 eq.), $PNSS_9$-N_3 (0.578 g, 0.180 mmol, 6 eq.), CuI (57 mg, 0.299 mmol, 10 eq.), DIPEA (diisopropylethylamine, 1 mL) and THF (20 mL) were charged to a 50 mL round-bottomed flask, evacuated for 10 minutes and backfilled with nitrogen (3 cycles). The flask was then kept at 50 °C for 5 days, following which, the solution was passed through a neutral alumina column to remove the copper catalyst. After concentrating the solution *in vacuo*, the product was recovered by precipitation in methanol, dried under reduced pressure, and then subjected to soxhlet purification with methanol and acetone, respectively. The product was finally extracted with chloroform, concentrated under reduced pressure and dried under vacuum overnight to yield the block copolymer.

Synthesis of poly(3-hexylthiophene)-*block*-poly(*p*-styrene sulfonate) (P3HT-*b*-PSS), 5, via thermal deprotection of P3HT-*b*-PNSS

30 mg of $P3HT_{50}$-*b*-$PNSS_x$ was added to a 1 mL glass vial. The vial was placed on a hotplate and covered with a funnel to which a nitrogen flow was applied. Each sample was heated at 150 °C for 3 hours before the polymer was removed from the hotplate and allowed to cool to room temperature.

Device fabrication

For this specific interlayer application, a "normal" device configuration was chosen. This device configuration allows the deprotection process of PNSS to be easily applied without affecting the

morphology of the photoactive layer. Before the layers were processed, the glass/ITO substrate was cleaned in an ultrasonic bath of acetone and propan-2-ol for 15 minutes each. Following cleaning, the substrates were dried and treated by UV-ozone for 10 minutes. PEDOT:PSS, used as a hole transporting layer, was subsequently coated directly from the commercial aqueous dispersion and dried at 130 °C in air for 5 min. A thin layer of P3HT-*b*-PNSS interfacial layer (0.5 mg/mL in chloroform) was then subsequently coated on top. Prior to coating the photoactive layer, the samples were heated for 3 hours at 150 °C in a controlled nitrogen atmosphere (glove-box). Following the thermal deprotection process, approximately 250 nm of P3HT:PCBM (1:0.8 w/w) photoactive layer was then coated on top of the interlayer. All layers were coated using a doctor blade. The devices were then completed by thermally evaporating 20 nm of Ca electrode and 500 nm of Ag (used as a protection layer to Ca) on customized mask. Before the evaporation of the metal electrode, the photoactive layer was annealed in nitrogen at 140 °C for 5 minutes.

CHARACTERIZATION

The monomer and polymer structures were characterized by ^{1}H NMR spectroscopy (in $CDCl_3$) using a Bruker Avance Spectrometer at 300 MHz. ^{1}H NMR spectroscopy was further used as an absolute method of determining M_n and the resultant degree of polymerization of P3HT. Relative M_n and dispersity (M_w/M_n, $Đ$) values were measured by Gel Permeation Chromatography (GPC) (flow rate 1 mL/min, 40 ^{o}C) using an Agilent 1100 Series GPC system, comprising two PL gel 10 µm 300 x 7.5 mm mixed-B columns and one PL gel 5 µm 300 x 7.5 mm mixed-C column and a degassed THF eluent system containing triethylamine (2 % v/v) and BHT (0.05 % w/v). The samples were calibrated with narrow polystyrene standards (M_p range = 162 to 6 035 000 g/mol) and analyzed using GPC Analysis software supplied by Agilent Technologies. Fourier transform

infrared (FTIR) spectra were obtained using attenuated total reflectance (ATR) on a Thermo Nicolet 380 FTIR spectrophotometer over the range 4000-500 cm^{-1} for 32 scans with a resolution of 4 cm^{-1} and the spectra were analyzed using Omnic software. Matrix Assisted Laser Desorption Ionisation Spectroscopy with Time of Flight detection Mass Spectroscopy (MALDI-ToF MS) measurements were performed at the University of Birmingham, UK, on a Waters Micromass micro MX using positive reflectron mode with dithranol as a matrix. The optical microscopy images have been taken with a LEICA DM LM Composed Optical Microscope equipped with a LEICA DFC280 camera in transmission and reflection modes.

Atomic force microscopy (AFM) and Grazing Incidence Small and Wide Angle X-ray Scattering (GISAXS/GIWAXS)

Samples were dissolved in THF (10 mg mL^{-1}) and spin-coated onto polished silicon wafers at 2000 rpm, before thermal treatment at 150 °C for 3 hours under an argon or nitrogen atmosphere. The surface topography of the prepared samples was analyzed through atomic force microscopy (AFM) (Park Systems, XE-100) under ambient conditions. Scans were performed in non-contact mode with enhanced resolution, silicon micro-cantilever tips. Topographic and phase images were recorded at a resonance frequency of approximately 270 kHz. For bulk morphological characterization, GISAXS/GIWAXS was employed on I07 (λ = 0.992 Å, sample to detector distance of 3.0 m using a Pilatus 2M 1475 × 1679 pixel detector with pixel size 172 μm) at the Diamond Light Source, Rutherford, UK and the BM26B-DUBBLE beamline (λ = 1.033 Å, sample to detector distance of 2.1 m using a Pilatus 1M 981 × 1043 pixel detector with pixel size 172 μm) at the European Synchrotron Radiation Facility (ESRF), Grenoble, France.[92, 93] 2D x-ray data was horizontally integrated for $q < 0.25$ $Å^{-1}$ to obtain 1D data for the small-angle in-

plane features and vertically integrated for $q > 0.25$ Å^{-1} to obtain 1D data for the wide-angle out-of-plane crystalline feature.

Device characterization

Cells were illuminated with a simulated solar spectrum from Steuernagel Solartest 1200 Oriel solar simulator at 100 mW/cm^2. The current density – voltage (*J-V*) characteristics of the devices were recorded using Keithley 2400 SMU in combination with Keithley 7001 Multiplexer system and custom software. The mismatch in the simulated solar spectrum is corrected by measuring the external quantum efficiency (EQE) of each cell.

RESULTS AND DISCUSSION

Synthesis of ethynyl-terminated regioregular poly(3-hexylthiophene) (P3HT$_{50}$-ethynyl), 2

Regioregular P3HT was prepared from 2,3-dibromo-3-hexylthiophene and isopropylmagnesium chloride via Ni-catalysed Grignard metathesis (GRIM) polymerization according to the literature.[84] To equip P3HT with a 'clickable' moiety, an ethynyl end group was introduced to the homopolymer through the addition of ethynylmagnesium bromide at the end of the polymerization. The polymer (dissolved in chloroform) was precipitated several times from methanol and the high purity of the final homopolymer was confirmed by ^{1}H NMR spectroscopy (Figure S1). MALDI-ToF was also used to confirm the presence of the alkyne-functionality (Figure S2). Table 1 shows the molar mass data for the P3HT$_{50}$-ethynyl homopolymer, indicating good control over the molar mass distribution ($Đ = 1.23$), as expected with GRIM polymerization of thiophene monomers. Interestingly, ^{1}H NMR spectroscopy reveals a P3HT degree of polymerization of 50, whereas MALDI-ToF suggests an average D_p of around 37 and

GPC indicates one of 75, although all three methods are known to give rise to inaccuracies in these measurements. Specifically, McCullough *et al.*[94] showed that molar masses calculated by GPC analyses are higher for poly(alkylthiophenes) than those obtained by MALDI characterization by a factor of 1.2 to 2.3 times, commensurate with our data here (2.0 times higher). Consequently, a value of 50 has been used throughout this study for simplicity purposes only. This issue is further discussed with the GISAXS data (*vide infra*). It is noteworthy that P3HT-ethynyl was highly sensitive to the purification and storage conditions used. GPC (Figure 1) showed that the major P3HT product had a low molar mass dispersity, with a small high molar mass shoulder. This trace impurity is attributed to alkyne-alkyne coupling occurring in the presence of metal catalyst residues.[95] Rather than remove the P3HT impurity at this stage, the polymer product was used directly in the click reaction with PNSS-N_3 and then unreacted P3HT could be removed more readily following coupling (*vide infra*).

Synthesis of azide-terminated poly(neopentyl *p*-styrene sulfonate) (PNSS-N_3), 4

The azide entity in our click coupling reaction was PNSS-N_3, with varying degrees of polymerization. This block was prepared by the RAFT polymerization of neopentyl *p*-styrene sulfonate (NSS, **3**), using azide terminated chain transfer agent, 2-dodecylsulfanylthiocarbonylsulfanyl-2-methyl propionic acid 2-azido-ethyl ester (CTA-N_3) and AIBN in anisole (50 % w/v) at 80 °C for 26 hours. A series comprising three PNSS-N_3 homopolymers was readily synthesized by adjusting the monomer to CTA ratio (targeting D_p = 10, 20 and 30). Table 1 shows that our RAFT system is well-suited for the controlled polymerization of NSS monomer, yielding polymers with low molar mass dispersities ($Đ \leq 1.20$, monomer conversion ~ 80 %) over a range of molar masses. The achieved degrees of

polymerisation, noted as 9, 16 and 23, respectively, have been calculated from the data obtained from GPC analyses and, although relative to PS standards, are in good agreement with 80 % (monomer conversion) of the targeted values. It should be noted that, ^{1}H NMR spectroscopy, often used to calculate a more accurate D_p value for low molar mass polymers via end-group analysis, could not be employed in this case; peaks obtained within the region of the different CTA protons were not in agreement with one another.

Table 1. Molar mass data of the three P3HT-*b*-PNSS block copolymers, synthesized by azide-alkyne click chemistry, and their corresponding homopolymer building blocks.

Polymer	M_n[a]	**Đ** (M_w/M_n)	**Yield**
$P3HT_{50}$-ethynyl	12 600	1.23	52 %
$PNSS_9$-N_3	2 600	1.12	72 %
$PNSS_{16}$-N_3	4 600	1.15	84 %
$PNSS_{23}$-N_3	6 200	1.20	84 %
$P3HT_{50}$-*b*-$PNSS_9$	15 000	1.22	72 %
$P3HT_{50}$-*b*-$PNSS_{16}$	18 800	1.27	84 %
$P3HT_{50}$-*b*-$PNSS_{23}$	19 600	1.45	77 %

(a) Determined by THF GPC against polystyrene standards.

Synthesis of poly(3-hexylthiophene)-*block*-poly(neopentyl *p*-styrene sulfonate) (P3HT-*b*-PNSS)

Copper-catalyzed azide-alkyne click chemistry was employed to couple $P3HT_{50}$-ethynyl with $PNSS_x$-N_3 to afford a small series of block copolymers where the PNSS block length has been systematically varied. To ensure complete conversion of the more labour-intensive P3HT block, the relatively inexpensive PNSS block was added in large excess. The success of the azide-alkyne click coupling was confirmed by ^{1}H NMR spectroscopy; the spectra of P3HT-*b*-PNSS with varying PNSS lengths are shown in Figure 2 and Figures S6 and S7. Indeed, all peaks corresponding to PNSS (7.71 ppm, 4.48 ppm 3.77 and 3.23 ppm) and P3HT (6.97 ppm, 2.80 ppm, 1.70 ppm, 1.35 ppm and 0.91 ppm) are present in the spectra of the block copolymers. In addition, the peak in the P3HT spectrum arising from the alkyne proton (at 3.52 ppm) has completely disappeared. A peak arising from the proton on the triazole ring (h) of the cycloaddition product is observed at 7.67 ppm in the spectrum of each block copolymer, however this signal is heavily masked by the peak corresponding to the aromatic protons of the styrene sulfonate repeat units. Nevertheless, GPC analysis of the diblock copolymers and corresponding building blocks (Figure 1 and Table 1) clearly demonstrate the expected increase in molar mass following the coupling reaction; 15 000, 18 800 and 19 600 $gmol^{-1}$ for $P3HT_{50}$-*b*-$PNSS_9$, $P3HT_{50}$-*b*-$PNSS_{16}$, $P3HT_{50}$-*b*-$PNSS_{23}$, respectively. Additionally, the traces show no PNSS homopolymer impurity, revealing that the PNSS content is covalently bound to P3HT and, furthermore, owing to the smooth GPC traces, the small amount of high molar mass P3HT (homo-coupled) impurity appears to have been mostly removed during the purification of the diblock copolymers.

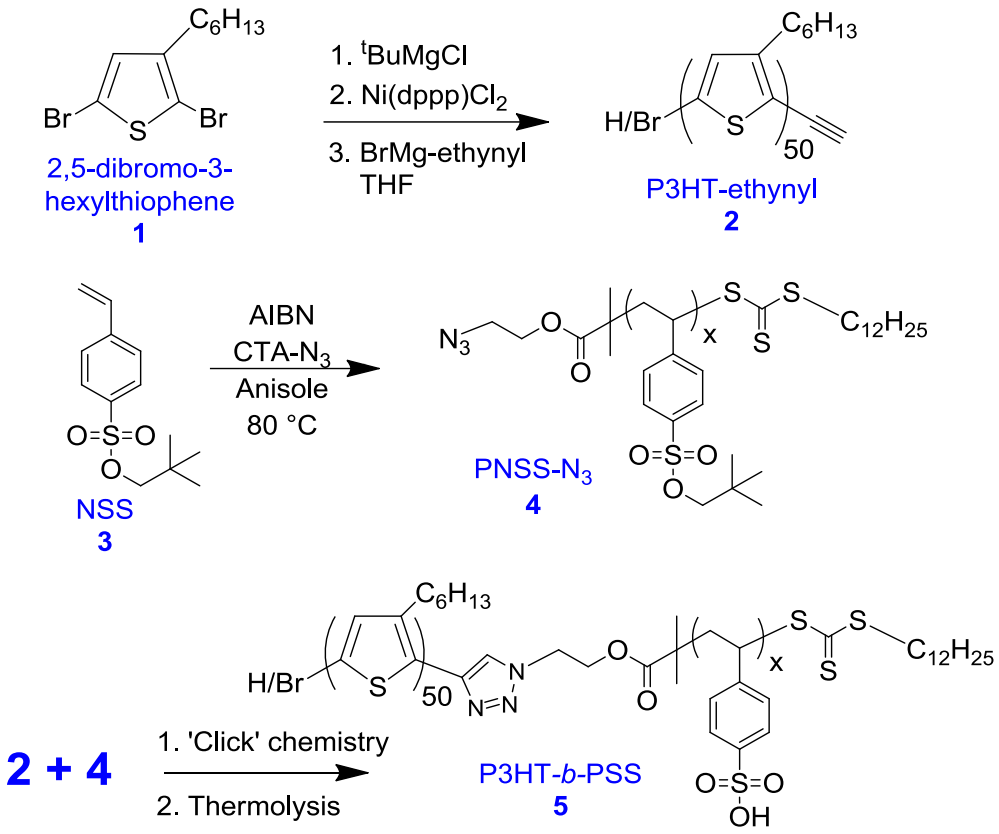

Scheme 1. Synthetic strategy for the preparation of P3HT-*b*-PSS.

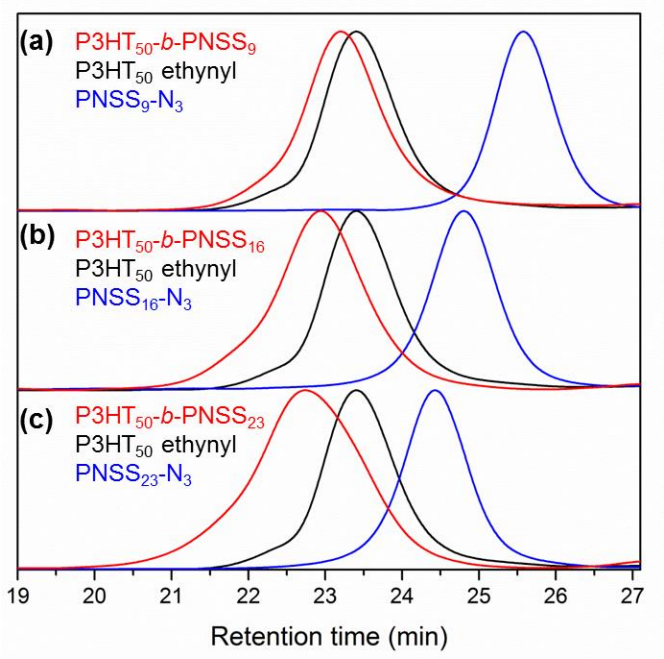

Figure 1. GPC traces of (a) $P3HT_{50}$-*b*-$PNSS_9$, $P3HT_{50}$-ethynyl and $PNSS_9$-N_3; (b) $P3HT_{50}$-*b*-$PNSS_{16}$, $P3HT_{50}$-ethynyl and $PNSS_{16}$-N_3; and (c) $P3HT_{50}$-*b*-$PNSS_{23}$, $P3HT_{50}$-ethynyl and $PNSS_{23}$-N_3.

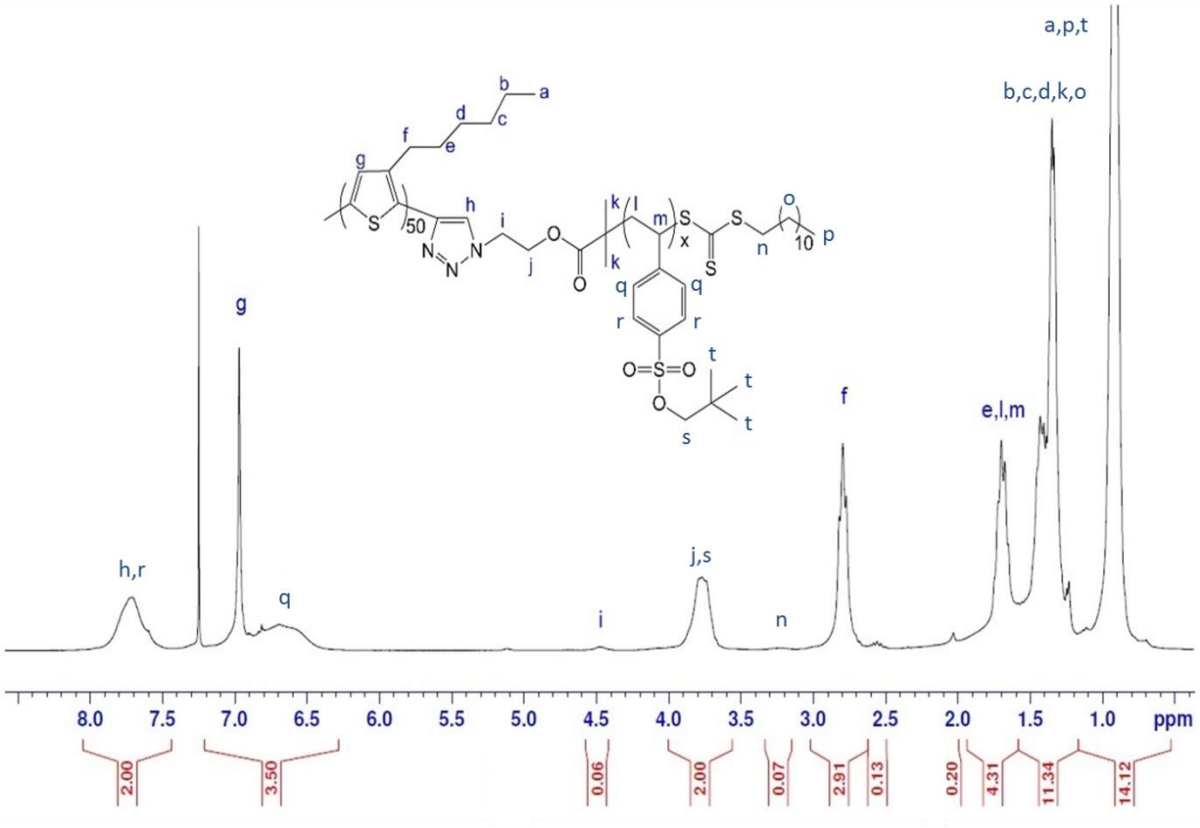

Figure 2. ^{1}H NMR spectrum of $P3HT_{50}$-*b*-$PNSS_{23}$ (300 MHz, $CDCl_3$).

Infrared spectroscopy further confirmed the successful formation of the three block copolymers. Figure 3 shows the FTIR spectrum of a representative diblock copolymer ($P3HT_{50}$-*b*-$PNSS_{23}$) and those of its corresponding homopolymer precursors (the FTIR spectra of other two block copolymers and their precursors are provided in the ESI, Figures S8 and S9). Indeed, the signal at 2100 cm^{-1}, arising from the azide functionality on $PNSS_{23}$-N_3 and the signals around 2100 cm^{-1} and 3300 cm^{-1}, corresponding to the acetylene group present on the $P3HT_{50}$-ethynyl polymer, are not present in the spectrum of the diblock copolymer, $P3HT_{50}$-*b*-$PNSS_{23}$, whilst the characteristic bands arising from the groups in both homopolymers are present.

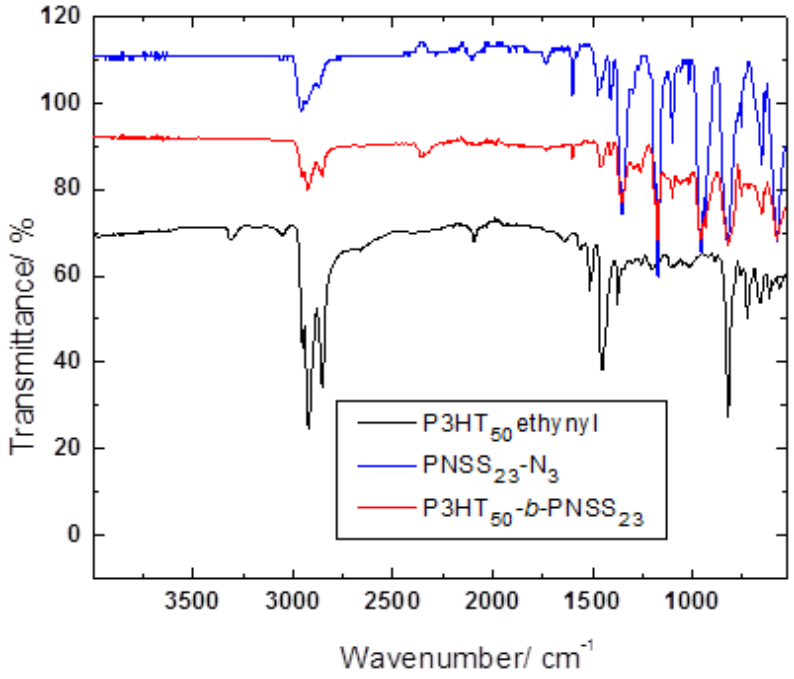

Figure 3. FTIR spectra of P3HT$_{50}$-*b*-PNSS$_{23}$, P3HT$_{50}$-ethynyl and PNSS$_{23}$-N$_3$.

Synthesis of poly(3-hexylthiophene)-*block*-poly(*p*-styrene sulfonate) (P3HT-*b*-PSS), 5, via thermal deprotection of P3HT-*b*-PNSS

The thermally-induced modification of our copolymers during annealing at 150 °C for three hours (under nitrogen) was assessed *in situ* by TGA, as shown in Figure 4. It is noteworthy that these annealing conditions were not sufficient for complete deprotection of the block copolymers with low PNSS contents. However, further annealing was not undertaken as three hours at 150 °C is already considered excessive for OPV device manufacture. The thermograms show clearly that the deprotection rate depends on the PNSS chain length, following the order: P3HT$_{50}$-*b*-PNSS$_{23}$ > P3HT$_{50}$-*b*-PNSS$_{16}$ > P3HT$_{50}$-*b*-PNSS$_9$. Interestingly, the presence of the more rigid P3HT block proved to have a major influence on the deprotection rate. As a direct comparison, TGA was performed on PNSS$_{23}$-N$_3$. The trace shows the removal of the neopentyl group after 45 minutes at 150 °C, whereas, under the same conditions, the deprotection of

P3HT$_{50}$-*b*-PNSS$_{23}$ requires 130 minutes of annealing. This is in line with the trend observed for our block copolymers, where the larger the volume fraction of P3HT (*i.e.* the shorter the PNSS block), the longer the required deprotection time. Furthermore, the results indicate that the Friedel-Crafts side reaction (where a significant number of protecting groups are removed to reveal the sulfonate groups but are not removed as a volatile by-product and instead rearrange to attach to the aromatic ring in the *meta* position), described for PNSS homopolymers,[75, 96] does not occur in the presence of P3HT, as the expected weight loss for P3HT$_{50}$-*b*-PNSS$_{23}$ (11 %) is similar to the observed experimental results (12 %). In the control herein (PNSS homopolymer), there is no P3HT to hinder the Friedel-Crafts acylation and so deprotection to 91 % is observed (9 % loss), rather than the theoretically expected 74 %.

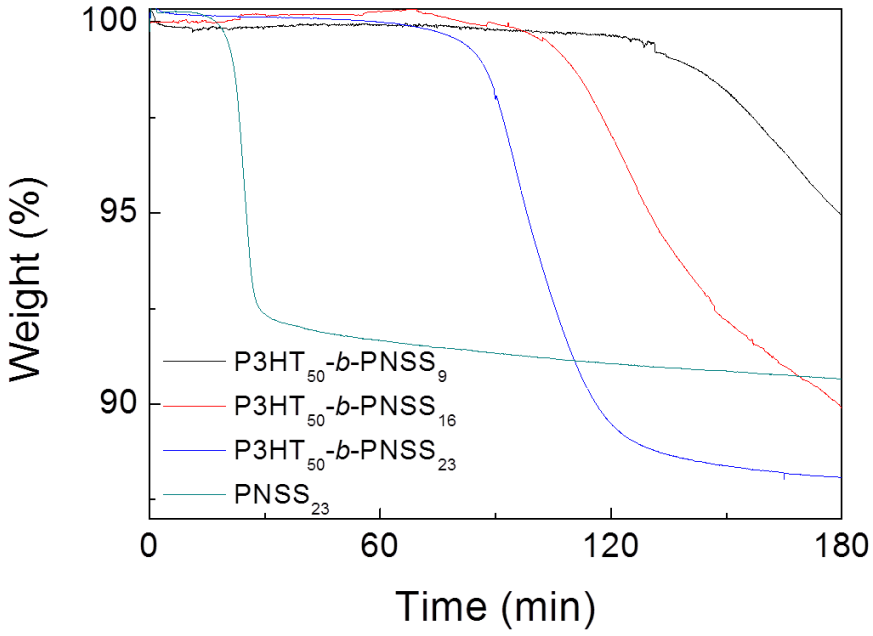

Figure 4. Thermogravimetric isotherms at 150 °C of the three P3HT$_{50}$-*b*-PNSS$_x$ block copolymers alongside PNSS$_{23}$ homopolymer as a control.

To compliment TGA, FTIR spectroscopy has been used to confirm that the observed weight loss indeed corresponds to the deprotection of the sulfonate groups in our block copolymers. Representative FTIR spectra of $P3HT_{50}$-*b*-$PNSS_{23}$, before and after annealing at 150 °C for three hours, are shown in Figure 5. As expected, a significant reduction in intensity of the band associated with saturated C-H stretching (from the alkyl chains, υ(C-H) ~ 2900 cm^{-1}) was clearly observed, whilst a broad band appeared in the region of 3250 cm^{-1}, indicative of the presence of the unprotected sulfonate group. This is in agreement with the observed changes in previous studies on PNSS homopolymers, where the transformation was followed by both FTIR and ^{1}H NMR spectroscopies.[75, 96] Accordingly, the FTIR spectra of $P3HT_{50}$-*b*-$PNSS_{9}$ and $P3HT_{50}$-*b*-$PNSS_{16}$ are provided in the ESI (Figures S10 and S11) and show similar changes to the ones highlighted herein, confirming that deprotection is occurring in all three diblock copolymers in our series.

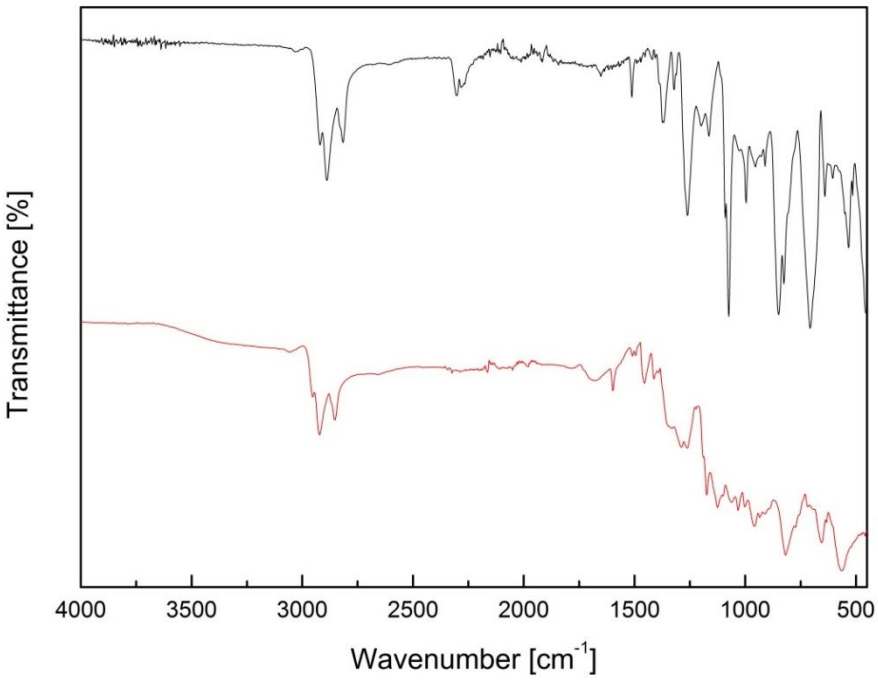

Figure 5. FTIR spectra of $P3HT_{50}$-*b*-$PNSS_{23}$ before (top) and after (bottom) thermal treatment (three hours at 150 °C). The spectra have been translated along the transmission axis for clarity purposes.

Thin film morphology of P3HT-*b*-PNSS and P3HT-*b*-PSS

First, the microscale morphology of our block copolymers was probed, before and after treatment, by optical microscopy (see Figure S12). The images clearly show long range liquid-like phase separation with domain widths of approximately 0.5 µm, independent of thermal treatment at 150 °C. However, for use in photovoltaic devices, the nanomorphology is of particular importance. Accordingly, Figure 6 shows the data obtained from GISAXS/GIWAXS (2D and corresponding integrated 1D) alongside tapping mode AFM images for spin-coated thin films (ca. 100 – 200 nm thick) of the three block copolymers, before and after annealing at 150 °C for three hours.

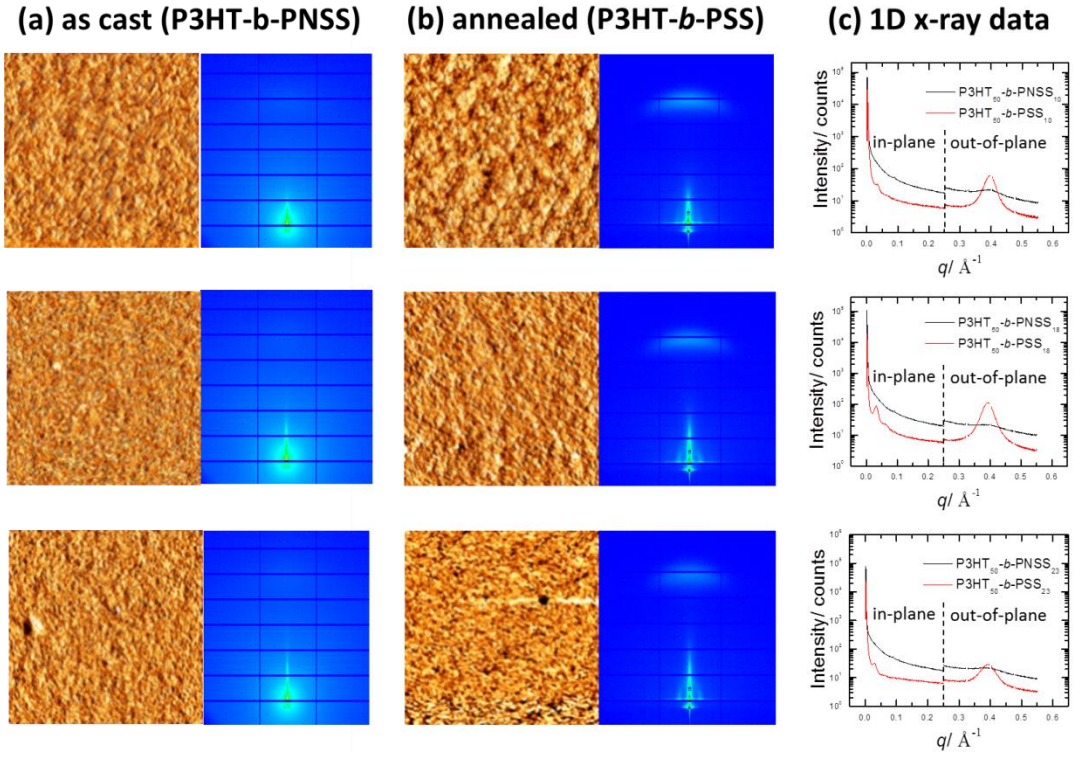

Figure 6. AFM phase images (2 × 2 microns) and 2D x-ray scattering raw data, as spin-coated (a) and after thermal annealing at 150 °C for 3 hours (b); and integrated 1D x-ray data (horizontal integration for $q < 0.25$ Å^{-1} and vertical integration for $q > 0.25$ Å^{-1} to highlight the in-plane and out-of-plane features, respectively- see Figure 7) (c) for P3HT-*b*-PNSS$_9$ (top), P3HT-*b*-PNSS$_{16}$ (middle) and P3HT-*b*-PNSS$_{23}$ (bottom).

Prior to thermal modification (and concomitant annealing), there was no microphase separation or clear definition between nanoscale domains and only negligible P3HT crystallinity for the block copolymers due to the spin-coating quench preventing appropriate alignment of the polymer chains. After annealing for 3 hours at 150 °C, the P3HT crystallinity is clearly visible for all diblock copolymers ($q = 0.397$ Å^{-1} for P3HT$_{50}$-*b*-PSS$_9$ and $q = 0.393$ Å^{-1} for both P3HT$_{50}$-*b*-PSS$_{16}$ and P3HT$_{50}$-*b*-PSS$_{23}$, corresponding to approximate length scales of 1.58 and 1.60 nm, respectively, in line with our pristine P3HT$_{50}$ homopolymer, see Figure S13, and the literature for P3HT packing with RR of 98 %[97]). This (100) peak in each case is indicative of the interchain spacing between the P3HT segments as they pack in the crystals (depicted by 'a' in Figure 7). Our data illustrate that this length scale is similar for the different PSS block lengths showing that the crystal packing of P3HT is not significantly perturbed by the presence of the covalently attached amorphous polymer segment, and appears unaffected above a certain molar mass. However, the approximate extent of crystallinity (quantity of crystalline domains; indicated by the intensity of the GIWAXS peak) is affected by the length of PSS, with the block copolymer with the highest amorphous PSS content, P3HT$_{50}$-*b*-PSS$_{23}$, showing considerably lower levels of crystallization. However, caution should be made in defining precise levels of crystallinity from these data as the intensity of the scattering peaks is also a function of the

quality of the alignment with respect to the critical angle for the air/silicon interface which can become slightly misaligned due to thermal expansion effects. As expected, P3HT packing is shown to be perpendicular to the lamellae stacks, revealed by the opposing orientations of the diffraction patterns at small and wide angles, respectively. It is noteworthy that our thermal treatment is above the glass transition temperature of both blocks (the more rigid P3HT having a T_g around 12 °C[98]), but considerably below the melting temperature of P3HT (T_m > 200 °C[99]). This allows moderate chain diffusion, but not significant rearrangement within the crystals to give substantial alignment of the P3HT repeat units [hence the presence of only a weak (100) peak in the GIWAXS data]. Figure 7 shows a cartoon schematic of the packing of the P3HT-*b*-PSS block copolymers following thermal treatment, based on the extensive work of Steiner and Hüttner with P3HT.[97, 100]

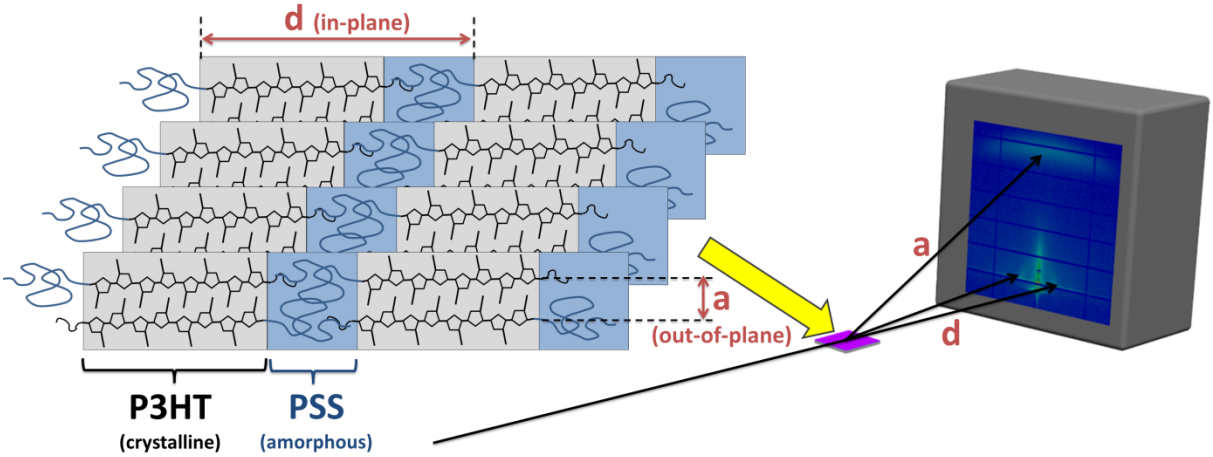

Figure 7. Schematic of the diblock copolymer molecular arrangement in our thin films, indicating the length scales measured by GISAXS/GIWAXS.

Solvent annealing the as cast block copolymers in THF vapour for 36 hours (see Figure S14, ESI) allowed a small amount of P3HT crystals to form (illustrated by the weak GIWAXS peak in all images), but did not produce a well-ordered periodic structure of crystalline and amorphous

domains. On the contrary, thermal deprotection of PNSS (to afford polar PSS) causes the Flory-Huggins interaction parameter, χ, between P3HT and the amorphous block to dramatically increase, inducing microphase separation, whilst concomitantly increasing the electron density contrast between the crystalline and amorphous domains. Indeed, following thermal treatment, distinct periodic structure (arising from crystalline and amorphous, highlighted by 'd' in Figure 7) is observed at $q^* = 0.0334$, 0.0320 and 0.0302 $Å^{-1}$ for P3HT-*b*-PSS_9, P3HT-*b*-PSS_{16} and P3HT-*b*-PSS_{23}, respectively. Thus, as PSS is increased (from approximately 9 to 16 to 23), the corresponding length scale between like domains increases from 18.8 to 19.7 to 20.8 nm. Given that the $P3HT_{50}$-alkyne homopolymer gave an inter-lamellae distance of approximately 17 nm (see Figure S13), the amorphous domains in the block copolymer series are 1.8, 2.7 and 3.8 nm, respectively. A plot of log *D* versus log *N* (Figure S15), where *D* is the amorphous domain length and *N* the approximate degree of polymerization of the amorphous segment, gives an approximate linear correlation with an alpha value of 0.79, in line with the literature, which states that $D \sim N^{\alpha}$, with $0.5 \leq \alpha \leq 1$.[101-105] In addition, a P3HT crystalline domain length of 17 nm suggests that our crystalline segments comprise of approximately 45 linear 3HT units (using 0.38 nm as the 3HT repeat unit spacing, as reported by Brinkmann and Rannou[106]), which closely matches the D_p of 50 estimated by ^{1}H NMR spectroscopy.

Interestingly, higher order Bragg peaks were observed at $2q^*$, most notably for P3HT-*b*-PSS_{16} and to a lesser extent for P3HT-*b*-PSS_9 (see ESI, Figure S16), to reveal lamellae morphologies for these block copolymers. In line with the work of Snyder *et al.*[107] and Kohn *et al.*,[97] our P3HT of 8.4 kg mol^{-1} (by ^{1}H NMR) gives fully extended crystals (i.e. no folds) as illustrated in the simplified schematic in Figure 7, and increasing the PSS content pushes these crystals further apart. The ability to control the domain spacing of the semi-crystalline P3HT blocks is useful in

balancing the charge carrier properties with other physical properties of the films. It is noteworthy that although the GISAXS data confirm the lamellar layers in the bulk of the film, the AFM images did not reveal clear detail on the surface (left hand column of Figure 6). This is attributed to the formation of a wetting layer on the surface caused by the vast difference in surface energy between the two polymer blocks (see ESI, Figures S17 to S19).

Preliminary OPV device performance

The investigation of our block copolymers incorporated into OPV devices to enhance their long-term stability is beyond the scope of the work herein and will be described in full in a later report. However, to demonstrate that the introduction of these novel block copolymers can be executed without detrimentally affecting OPV device performance, Figure 8 shows power conversion efficiencies for non-optimized devices (with and without the block copolymer interlayers before and after thermolysis) in a 'normal' architecture.

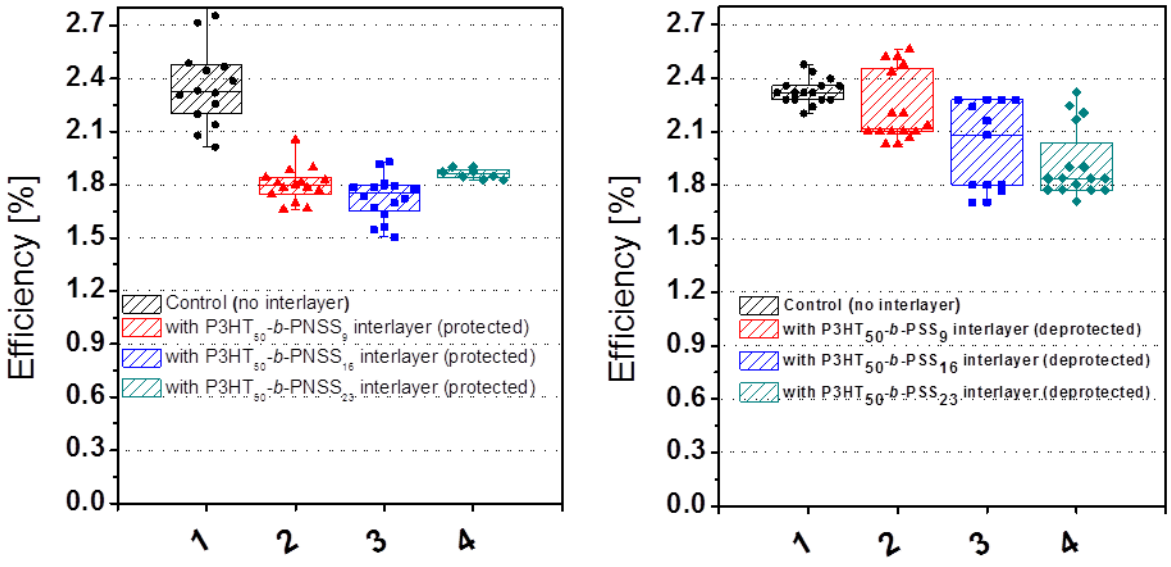

Figure 8. Power conversion efficiencies of ITO/PEDOT:PSS/interlayer/P3HT:PCBM/Ca/Ag devices before (a) and after (b) thermolysis of the block copolymer interlayer.

Figure 8 shows that introducing the block copolymer interlayer between a P3HT:PCBM photoactive layer and a PEDOT:PSS hole transport layer reduces the power conversion efficiency of non-optimized devices to approximately 75 % of the original value when the block copolymers are in the hydrophobic, protected forms. The extent of this reduction in device efficiency appears to be independent of the PNSS block length in our series. On the contrary, when the interlayers had been thermally treated to convert the PNSS blocks to PSS, the device efficiencies were not significantly affected by the presence of the shortest block copolymer, $P3HT_{50}$-*b*-PSS_9. The contributions of the block copolymer layer in terms of short circuit current (J_{SC}), injection, open circuit voltage (V_{OC}), fill factor and leakage, and the effect of block lengths will be discussed in detail in a further report.

CONCLUSIONS

A short series of novel poly(3-hexylthiophene)-*block*-poly(neopentyl *p*-styrene sulfonate), P3HT-*b*-PNSS, block copolymers with a P3HT block of fixed length attached to systematically varied PNSS block lengths, has been synthesized by GRIM and RAFT polymerization techniques, respectively, and subsequent azide-alkyne click coupling chemistry. The route is simple and affords pure block copolymers of relatively low molar mass dispersity ($Đ \leq 1.5$) with moderate overall yields. Importantly, these block copolymers can be processed from a single organic solvent and then rendered amphiphilic following thermolysis (150 °C). Thermolysis of the sulfonate ester removed the neopentyl protecting groups to produce P3HT-*block*-poly(*p*-styrene sulfonate), P3HT-*b*-PSS. TGA revealed that block copolymers with higher PNSS

contents required shorter processing times, despite more protecting groups requiring removal. GISAXS/GIWAXS was used to probe the nanomorphology and crystallinity of spin-coated thin films of the block copolymers before and after thermal modification. Prior to thermolysis, none of the polymers demonstrated long range order on the nanoscale with only minimal P3HT crystallinity, owing to vitrification of the polymers during the spin-coating process. However, following deprotection of PNSS and concomitant rearrangement of the chains at elevated temperature, the P3HT crystallinity increased and lamellar nanomorphologies were observed. Interestingly, the spacing between the P3HT lamellae was systematically increased on increasing the original PNSS block length. The ability to control the domain spacing of the semi-crystalline P3HT blocks is useful in balancing the charge carrier properties with other physical properties of the films.

ASSOCIATED CONTENT

Supporting Information.

Further experimental details, ^{1}H NMR, FTIR spectra of the block copolymers, MALDI ToF spectrum of P3HT$_{50}$-alkyne, optical microscopy images of P3HT$_{50}$-PNSS$_{9}$, 2D GISAXS/GIWAXS images for P3HT$_{50}$-alkyne (thermally annealed) and the block copolymers (solvent annealed), log D versus log N (taken from the x-ray data, more detailed plots of the 1D GISAXS profiles for the block copolymers, contact angle images and AFM images of the block copolymers. This material is available free of charge via the Internet at http://pubs.acs.org.

AUTHOR INFORMATION

Corresponding Author

*E-mail p.d.topham@aston.ac.uk

Author Contributions

The manuscript was written through contributions of all authors. All authors have given approval to the final version of the manuscript.

Funding Sources

The research leading to these results has received funding from the European Union Seventh Framework Programme (FP7/2010 SYNABCO n° 273316 and FP7/2011 under grant agreement ESTABLIS n° 290022).

ACKNOWLEDGMENT

The research leading to these results has received funding from the European Union Seventh Framework Programme (FP7/2010 SYNABCO n° 273316 and FP7/2011 under grant agreement ESTABLIS n° 290022). Thanks to Diamond Light Source and European Synchrotron Radiation Facility for providing beam time under allocations SI8536 and MA-2446, respectively. PDT thanks Mark Turner and Reese Lillie in the Aston University workshop for manufacture of the x-ray annealing rig and Jonathan Rawle for computer programming at the Diamond Light Source. Professor Yvonne Perrie and Jiteen Ahmed (School of Life & Health Sciences, Aston University) are thanked for their help with TGA measurements.

REFERENCES

1. Huang, Y.; Kramer, E. J.; Heeger, A. J.; Bazan, G. C. *Chemical Reviews* **2014,** 114, (14), 7006-7043.
2. Chamberlain, G. A. *Solar Cells* **1983,** 8, (1), 47-83.
3. Heeger, A. J. *Advanced Materials* **2014,** 26, (1), 10-28.
4. Li, G.; Zhu, R.; Yang, Y. *Nature Photonics* **2012,** 6, (3), 153-161.
5. Nelson, J. *Materials Today* **2011,** 14, (10), 462-470.
6. Bundgaard, E.; Krebs, F. C. *Solar Energy Materials and Solar Cells* **2007,** 91, (11), 954-985.
7. Günes, S.; Neugebauer, H.; Sariciftci, N. S. *Chemical Reviews* **2007,** 107, (4), 1324-1338.
8. Facchetti, A. *Materials Today* **2013,** 16, (4), 123-132.
9. Xu, T.; Yu, L. *Materials Today* **2014,** 17, (1), 11-15.
10. Boudreault, P.-L. T.; Najari, A.; Leclerc, M. *Chemistry of Materials* **2010,** 23, (3), 456-469.
11. Krebs, F. C. *Solar Energy Materials and Solar Cells* **2009,** 93, (4), 394-412.
12. Søndergaard, R. R.; Hösel, M.; Krebs, F. C. *Journal of Polymer Science Part B: Polymer Physics* **2013,** 51, (1), 16-34.
13. Tipnis, R.; Bernkopf, J.; Jia, S.; Krieg, J.; Li, S.; Storch, M.; Laird, D. *Solar Energy Materials and Solar Cells* **2009,** 93, (4), 442-446.
14. Lee, J. U.; Jung, J. W.; Jo, J. W.; Jo, W. H. *Journal of Materials Chemistry* **2012,** 22, (46), 24265-24283.
15. Rivaton, A.; Tournebize, A.; Gaume, J.; Bussière, P.-O.; Gardette, J.-L.; Therias, S. *Polymer International* **2014,** 63, (8), 1335-1345.
16. Jørgensen, M.; Norrman, K.; Krebs, F. C. *Solar Energy Materials and Solar Cells* **2008,** 92, (7), 686-714.
17. Fraga Domínguez, I.; Topham, P. D.; Bussiere, P.-O.; Bégué, D.; Rivaton, A. *The Journal of Physical Chemistry C* **2015**, DOI: 10.1021/jp5103065.
18. Chawdhury, N.; Köhler, A.; Harrison, M. G.; Hwang, D. H.; Holmes, A. B.; Friend, R. H. *Synthetic Metals* **1999,** 102, (1–3), 871-872.
19. Norrman, K.; Madsen, M. V.; Gevorgyan, S. A.; Krebs, F. C. *Journal of the American Chemical Society* **2010,** 132, (47), 16883-16892.
20. Turkovic, V.; Engmann, S.; Egbe, D. A. M.; Himmerlich, M.; Krischok, S.; Gobsch, G.; Hoppe, H. *Solar Energy Materials and Solar Cells* **2014,** 120, Part B, (0), 654-668.
21. Schaffer, C. J.; Palumbiny, C. M.; Niedermeier, M. A.; Jendrzejewski, C.; Santoro, G.; Roth, S. V.; Müller-Buschbaum, P. *Advanced Materials* **2013,** 25, (46), 6760-6764.
22. Norrman, K.; Larsen, N. B.; Krebs, F. C. *Solar Energy Materials and Solar Cells* **2006,** 90, (17), 2793-2814.
23. Krebs, F. C.; Norrman, K. *Progress in Photovoltaics: Research and Applications* **2007,** 15, (8), 697-712.
24. Lögdlund, M.; Brédas, J. L. *The Journal of Chemical Physics* **1994,** 101, (5), 4357-4364.
25. Dupont, S. R.; Voroshazi, E.; Heremans, P.; Dauskardt, R. H. *Organic Electronics* **2013,** 14, (5), 1262-1270.
26. Liao, H.-C.; Ho, C.-C.; Chang, C.-Y.; Jao, M.-H.; Darling, S. B.; Su, W.-F. *Materials Today* **2013,** 16, (9), 326-336.
27. Howard, I. A.; Mauer, R.; Meister, M.; Laquai, F. *Journal of the American Chemical Society* **2010,** 132, (42), 14866-14876.

28. Chen, L.-M.; Hong, Z.; Li, G.; Yang, Y. *Advanced Materials* **2009,** 21, (14-15), 1434-1449.
29. Topham, P. D.; Parnell, A. J.; Hiorns, R. C. *Journal of Polymer Science Part B: Polymer Physics* **2011,** 49, (16), 1131-1156.
30. Yassar, A.; Miozzo, L.; Gironda, R.; Horowitz, G. *Progress in Polymer Science* **2013,** 38, (5), 791-844.
31. Sun, Z.; Xiao, K.; Keum, J. K.; Yu, X.; Hong, K.; Browning, J.; Ivanov, I. N.; Chen, J.; Alonzo, J.; Li, D.; Sumpter, B. G.; Payzant, E. A.; Rouleau, C. M.; Geohegan, D. B. *Advanced Materials* **2011,** 23, (46), 5529-5535.
32. Yang, C.; Lee, J. K.; Heeger, A. J.; Wudl, F. *Journal of Materials Chemistry* **2009,** 19, (30), 5416-5423.
33. Shi, Y.; Li, F.; Chen, Y. *New Journal of Chemistry* **2013,** 37, (1), 236-244.
34. Boudouris, B. W.; Frisbie, C. D.; Hillmyer, M. A. *Macromolecules* **2007,** 41, (1), 67-75.
35. Botiz, I.; Darling, S. B. *Macromolecules* **2009,** 42, (21), 8211-8217.
36. de Boer, B.; Stalmach, U.; van Hutten, P. F.; Melzer, C.; Krasnikov, V. V.; Hadziioannou, G. *Polymer* **2001,** 42, (21), 9097-9109.
37. Gholamkhass, B.; Holdcroft, S. *Chemistry of Materials* **2010,** 22, (18), 5371-5376.
38. Dante, M.; Yang, C.; Walker, B.; Wudl, F.; Nguyen, T.-Q. *Advanced Materials* **2010,** 22, (16), 1835-1839.
39. Sary, N.; Richard, F.; Brochon, C.; Leclerc, N.; Lévêque, P.; Audinot, J.-N.; Berson, S.; Heiser, T.; Hadziioannou, G.; Mezzenga, R. *Advanced Materials* **2010,** 22, (6), 763-768.
40. Scherf, U.; Adamczyk, S.; Gutacker, A.; Koenen, N. *Macromolecular Rapid Communications* **2009,** 30, (13), 1059-1065.
41. Ohshimizu, K.; Ueda, M. *Macromolecules* **2008,** 41, (14), 5289-5294.
42. Zhang, Y.; Tajima, K.; Hirota, K.; Hashimoto, K. *Journal of the American Chemical Society* **2008,** 130, (25), 7812-7813.
43. Lai, Y.-C.; Ohshimizu, K.; Takahashi, A.; Hsu, J.-C.; Higashihara, T.; Ueda, M.; Chen, W.-C. *Journal of Polymer Science Part A: Polymer Chemistry* **2011,** 49, (12), 2577-2587.
44. Dai, C.-A.; Yen, W.-C.; Lee, Y.-H.; Ho, C.-C.; Su, W.-F. *Journal of the American Chemical Society* **2007,** 129, (36), 11036-11038.
45. Müller, C.; Goffri, S.; Breiby, D. W.; Andreasen, J. W.; Chanzy, H. D.; Janssen, R. A. J.; Nielsen, M. M.; Radano, C. P.; Sirringhaus, H.; Smith, P.; Stingelin-Stutzmann, N. *Advanced Functional Materials* **2007,** 17, (15), 2674-2679.
46. Müller, C.; Radano, C. P.; Smith, P.; Stingelin-Stutzmann, N. *Polymer* **2008,** 49, (18), 3973-3978.
47. Chen, H.; Chen, J.; Yin, W.; Yu, X.; Shao, M.; Xiao, K.; Hong, K.; Pickel, D. L.; Kochemba, W. M.; Kilbey Ii, S. M.; Dadmun, M. *Journal of Materials Chemistry A* **2013,** 1, (17), 5309-5319.
48. Erothu, H.; Sohdi, A. A.; Kumar, A. C.; Sutherland, A. J.; Dagron-Lartigau, C.; Allal, A.; Hiorns, R. C.; Topham, P. D. *Polymer Chemistry* **2013,** 4, (13), 3652-3655.
49. Chen, J.; Yu, X.; Hong, K.; Messman, J. M.; Pickel, D. L.; Xiao, K.; Dadmun, M. D.; Mays, J. W.; Rondinone, A. J.; Sumpter, B. G.; Kilbey Ii, S. M. *Journal of Materials Chemistry* **2012,** 22, (26), 13013-13022.
50. Gu, Z.; Kanto, T.; Tsuchiya, K.; Shimomura, T.; Ogino, K. *Journal of Polymer Science Part A: Polymer Chemistry* **2011,** 49, (12), 2645-2652.

51. Patel, S. N.; Javier, A. E.; Stone, G. M.; Mullin, S. A.; Balsara, N. P. *ACS Nano* **2012,** 6, (2), 1589-1600.
52. Park, J.; Moon, H. C.; Kim, J. K. *Journal of Polymer Science Part A: Polymer Chemistry* **2013,** 51, (10), 2225-2232.
53. Lee, Y. J.; Kim, S. H.; Yang, H.; Jang, M.; Hwang, S. S.; Lee, H. S.; Baek, K.-Y. *The Journal of Physical Chemistry C* **2011,** 115, (10), 4228-4234.
54. Iovu, M. C.; Craley, C. R.; Jeffries-El, M.; Krankowski, A. B.; Zhang, R.; Kowalewski, T.; McCullough, R. D. *Macromolecules* **2007,** 40, (14), 4733-4735.
55. Saleh, M. M. *Desalination* **2009,** 235, (1–3), 319-329.
56. Rivard, A.; Raup, S.; Beilman, G. *Journal of Parenteral and Enteral Nutrition* **2004,** 28, (2), 76-78.
57. Simoes, J. A.; Citron, D. M.; Aroutcheva, A.; Anderson, R. A.; Chany II, C. J.; Waller, D. P.; Faro, S.; Zaneveld, L. J. D. *Antimicrobial Agents and Chemotherapy* **2002,** 46, (8), 2692-2695.
58. Girard, J.; Brunetto, P. S.; Braissant, O.; Rajacic, Z.; Khanna, N.; Landmann, R.; Daniels, A. U.; Fromm, K. M. *Comptes Rendus Chimie* **2013,** 16, (6), 550-556.
59. Yu, J.; Yi, B.; Xing, D.; Liu, F.; Shao, Z.; Fu, Y.; Zhang, H. *Physical Chemistry Chemical Physics* **2003,** 5, (3), 611-615.
60. Li, G.; Shrotriya, V.; Huang, J.; Yao, Y.; Moriarty, T.; Emery, K.; Yang, Y. *Nature Materials* **2005,** 4, (11), 864-868.
61. Ma, W.; Yang, C.; Gong, X.; Lee, K.; Heeger, A. J. *Advanced Functional Materials* **2005,** 15, (10), 1617-1622.
62. Lövenich, W. *Polym. Sci. Ser. C* **2014,** 56, (1), 135-143.
63. Wang, G.-F.; Tao, X.-M.; Wang, R.-X. *Composites Science and Technology* **2008,** 68, (14), 2837-2841.
64. Levermore, P. A.; Jin, R.; Wang, X.; Chen, L.; Bradley, D. D. C.; de Mello, J. C. *Journal of Materials Chemistry* **2008,** 18, (37), 4414-4420.
65. Do, H.; Reinhard, M.; Vogeler, H.; Puetz, A.; Klein, M. F. G.; Schabel, W.; Colsmann, A.; Lemmer, U. *Thin Solid Films* **2009,** 517, (20), 5900-5902.
66. Kim, Y. H.; Sachse, C.; Machala, M. L.; May, C.; Müller-Meskamp, L.; Leo, K. *Advanced Functional Materials* **2011,** 21, (6), 1076-1081.
67. Higashihara, T.; Ueda, M. *Macromolecular Research* **2013,** 21, (3), 257-271.
68. Dennler, G.; Scharber, M. C.; Brabec, C. J. *Advanced Materials* **2009,** 21, (13), 1323-1338.
69. Chu, T.-Y.; Alem, S.; Verly, P. G.; Wakim, S.; Lu, J.; Tao, Y.; Beaupré, S.; Leclerc, M.; Bélanger, F.; Désilets, D.; Rodman, S.; Waller, D.; Gaudiana, R. *Applied Physics Letters* **2009,** 95, (6), -.
70. Boudreault, P.-L. T.; Beaupre, S.; Leclerc, M. *Polymer Chemistry* **2010,** 1, (2), 127-136.
71. Roncali, J. *Chemical Society Reviews* **2005,** 34, (6), 483-495.
72. Bertho, S.; Janssen, G.; Cleij, T. J.; Conings, B.; Moons, W.; Gadisa, A.; D'Haen, J.; Goovaerts, E.; Lutsen, L.; Manca, J.; Vanderzande, D. *Solar Energy Materials and Solar Cells* **2008,** 92, (7), 753-760.
73. Yang, X.; van Duren, J. K. J.; Janssen, R. A. J.; Michels, M. A. J.; Loos, J. *Macromolecules* **2004,** 37, (6), 2151-2158.
74. Baek, K.-Y. *Journal of Polymer Science Part A: Polymer Chemistry* **2008,** 46, (18), 5991-5998.

75. Baek, K.-Y.; Kim, H.-J.; Lee, S.-H.; Cho, K.-Y.; Kim, H. T.; Hwang, S. S. *Macromolecular Chemistry and Physics* **2010,** 211, (6), 613-617.
76. Brendel, J. C.; Burchardt, H.; Thelakkat, M. *Journal of Materials Chemistry* **2012,** 22, (46), 24386-24393.
77. Semsarilar, M.; Perrier, S. *Nature Chemistry* **2010,** 2, (10), 811-820.
78. Fielding, L. A.; Derry, M. J.; Ladmiral, V.; Rosselgong, J.; Rodrigues, A. M.; Ratcliffe, L. P. D.; Sugihara, S.; Armes, S. P. *Chemical Science* **2013,** 4, (5), 2081-2087.
79. Pullan, N.; Liu, M.; Topham, P. D. *Polymer Chemistry* **2013,** 4, (7), 2272-2277.
80. Moad, G.; Rizzardo, E.; Thang, S. H. *Chemistry – An Asian Journal* **2013,** 8, (8), 1634-1644.
81. Isakova, A.; Topham, P. D.; Sutherland, A. J. *Macromolecules* **2014,** 47, (8), 2561-2568.
82. Warren, N. J.; Mykhaylyk, O. O.; Mahmood, D.; Ryan, A. J.; Armes, S. P. *Journal of the American Chemical Society* **2013,** 136, (3), 1023-1033.
83. Chaduc, I.; Lansalot, M.; D'Agosto, F.; Charleux, B. *Macromolecules* **2012,** 45, (3), 1241-1247.
84. Jeffries-El, M.; Sauvé, G.; McCullough, R. D. *Macromolecules* **2005,** 38, (25), 10346-10352.
85. Binder, W. H.; Sachsenhofer, R. *Macromolecular Rapid Communications* **2007,** 28, (1), 15-54.
86. Agut, W.; Taton, D.; Lecommandoux, S. *Macromolecules* **2007,** 40, (16), 5653-5661.
87. Vogt, A. P.; Sumerlin, B. S. *Macromolecules* **2006,** 39, (16), 5286-5292.
88. Urien, M.; Erothu, H.; Cloutet, E.; Hiorns, R. C.; Vignau, L.; Cramail, H. *Macromolecules* **2008,** 41, (19), 7033-7040.
89. Vora, A.; Singh, K.; Webster, D. C. *Polymer* **2009,** 50, (13), 2768-2774.
90. Okamura, H.; Takatori, Y.; Tsunooka, M.; Shirai, M. *Polymer* **2002,** 43, (11), 3155-3162.
91. Fraga Domínguez, I.; Kolomanska, J.; Johnston, P.; Rivaton, A.; Topham, P. D. *Polymer International* **2015**, DOI:10.1002/pi.4840.
92. Bras, W.; Dolbnya, I. P.; Detollenaere, D.; van Tol, R.; Malfois, M.; Greaves, G. N.; Ryan, A. J.; Heeley, E. *Journal of Applied Crystallography* **2003,** 36, 791-794.
93. Smilgies, D. M.; Busch, P.; Papadakis, C. M.; Posselt, D. *Synchrotron Radiation News* **2002,** 15, (5), 35-42.
94. Liu, J.; Loewe, R. S.; McCullough, R. D. *Macromolecules* **1999,** 32, (18), 5777-5785.
95. Li, Z.; Ono, R. J.; Wu, Z.-Q.; Bielawski, C. W. *Chemical Communications* **2011,** 47, (1), 197-199.
96. Li, X.; Jiang, Y.; Shuai, L.; Wang, L.; Meng, L.; Mu, X. *Journal of Materials Chemistry* **2012,** 22, (4), 1283-1289.
97. Kohn, P.; Rong, Z.; Scherer, K. H.; Sepe, A.; Sommer, M.; Müller-Buschbaum, P.; Friend, R. H.; Steiner, U.; Hüttner, S. *Macromolecules* **2013,** 46, (10), 4002-4013.
98. Zhao, Y.; Yuan, G. X.; Roche, P.; Leclerc, M. *Polymer* **1995,** 36, (11), 2211-2214.
99. Kim, Y.; Cook, S.; Tuladhar, S. M.; Choulis, S. A.; Nelson, J.; Durrant, J. R.; Bradley, D. D. C.; Giles, M.; McCulloch, I.; Ha, C. S.; Ree, M. *Nature Materials* **2006,** 5, (3), 197-203.
100. Sepe, A.; Rong, Z.; Sommer, M.; Vaynzof, Y.; Sheng, X.; Muller-Buschbaum, P.; Smilgies, D.-M.; Tan, Z.-K.; Yang, L.; Friend, R. H.; Steiner, U.; Huttner, S. *Energy & Environmental Science* **2014,** 7, (5), 1725-1736.
101. Kim, S.; Nealey, P. F.; Bates, F. S. *Nano Letters* **2013,** 14, (1), 148-152.

102. Matsushita, Y.; Mori, K.; Saguchi, R.; Nakao, Y.; Noda, I.; Nagasawa, M. *Macromolecules* **1990,** 23, (19), 4313-4316.
103. Hashimoto, T.; Shibayama, M.; Kawai, H. *Macromolecules* **1980,** 13, (5), 1237-1247.
104. Hashimoto, T.; Tsukahara, Y.; Kawai, H. *Polym J* **1983,** 15, (10), 699-711.
105. Hiorns, R. C.; Martinez, H. *Synthetic Metals* **2003,** 139, (2), 463-469.
106. Brinkmann, M.; Rannou, P. *Macromolecules* **2009,** 42, (4), 1125-1130.
107. Snyder, C. R.; Nieuwendaal, R. C.; DeLongchamp, D. M.; Luscombe, C. K.; Sista, P.; Boyd, S. D. *Macromolecules* **2014,** 47, (12), 3942-3950.

GRAPHICAL ABSTRACT

A series of novel block copolymers, which are transformed from hydrophobic to amphiphilic materials by external remote triggering, have been shown to form lamellae morphologies in thin films following thermal treatment.